Scientific Contributions Oil & Gas, Vol. 48. No. 4, December: 61 - 75

SCIENTIFIC CONTRIBUTIONS OIL AND GAS

Testing Center for Oil and Gas
LEMIGAS

Journal Homepage:http://www.journal.lemigas.esdm.go.id
ISSN: 2089-3361, e-ISSN: 2541-0520

# Improvement of Operating Performance of Medium-Speed Marine Diesel Engines Using Marine Diesel Oil with Air Microbubbles

Hideo Kawahara[1], Tomohiro Sunada[2], Yasuhito Nakatake[3], Koichi Terasaka[4], Hiroshi Kawahara[5], and Hidechika Goto[5]

[1]School of Systems Engineering, Department of Mechanical System Engineering, National Defense Academy
1-10-20 Hashirimizu, Yokosuka, Kanagawa, 2398686, Japan.

[2]Technical Support Center, National Institute of Technology, Oshima College
1091-1 Komatsu, Suo-Oshima, Oshima Yamaguchi, 7422193, Japan.

[3]Department of Mechanical Engineering, National Institute of Technology, Kurume College
1-1-1 Komorino, Kurume, Fukuoka, 8308555, Japan.

[4]Faculty of Science and Technology, Department of Applied Chemistry, Keio University
3-14-1 Hiyoshi, Kohoku-ku, Yokohama, Kanagawa, 2238522, Japan.

[5]Mes Tokki & Engineering Co., Ltd.
3-1-1 Tama, Tamano, Okayama, 7068651, Japan.

Corresponding author: Hideo Kawahara (kawahara@nda.ac.jp)

Manuscript received: October 10th, 2025; Revised: October 27th, 2025
Approved: October 29th, 2025; Available online: December 09th, 2025; Published: December 09th, 2025.

**ABSTRACT** - Marine diesel engines are widely adopted as the main auxiliary engines in ships because of their ability to utilize inexpensive heavy fuel oil and their high thermal efficiency per unit engine. This study focuses on practical marine medium-speed diesel engines to investigate the impact of introducing air as fine bubbles into low-sulfur A heavy fuel oil on the operating performance. The results indicated that when fine bubbles were introduced into the fuel, the engine exhibited poor combustion and became unstable at any load when $Q_a$ was 0.4 L/min or higher. However, when $Q_a$ was below 0.4 L/min, the fuel efficiency improvement increased significantly with increasing load, reaching a maximum reduction of 4.5% at 75% load and $Q_a$ = 0.3 L/min. Regarding the exhaust gas characteristics, at low loads, no significant changes were observed in the $CO_2$ and NOx emissions with varying microbubble injection levels. However, at loads of 75% or higher, both the $CO_2$ and NOx emissions decreased as the microbubble injection level increased. Furthermore, introducing fine bubbles into the fuel promoted atomization after fuel injection, similar to the results for heated C heavy oil, leading to improved heat generation rates across the entire engine load range.

**Keywords:** microbubbles, marine diesel engines, fuel consumption, cylinder pressure, heat generation rate.

**How to cite this article:**

Hideo Kawahara, Tomohiro Sunada, Yasuhito Nakatake, Koichi Terasaka, Hiroshi Kawahara, and Hidechika Goto, 2025, Improvement of Operating Performance of Medium-Speed Marine Diesel Engines Using Marine Diesel Oil with Air Microbubbles, Scientific Contributions Oil and Gas, 48 (4) pp. 61-75. DOI org/10.29017/scog.v48i4.1908.

## INTRODUCTION

Countries worldwide are successively declaring bans on the production and sale of diesel and gasoline vehicles that use fossil fuels. Following the automotive industry, the shipping sector is also experiencing a full-scale shift away from traditional heavy-fuel oils. Accelerating this shift was the International maritime organization (IMO)'s tightening of exhaust gas regulations by the International Maritime Organisation. Nitrogen oxides (NOx), sulfur oxides (SOx), and particulate matter (PM), which cause air pollution and lead to health hazards such as respiratory diseases, are regulated globally. The IMO regulates these pollutants in ships under the MARPOL 73/78 Convention (IMO 2022). Annex VI of this convention imposes fuel oil sulfur content (SOx) regulations to reduce SOx emissions. While the sulfur content was previously capped at 3.5% in general water, it was significantly lowered to 0.5% or less starting in January 2020. In addition to these air pollution measures, the Paris Agreement, reached at the 21st Conference of the Parties (COP21) to the United Nations Framework Convention on Climate Change (UNFCCC) in 2015, established a global long-term goal to limit the increase in the global average temperature to below 2°C above pre-industrial levels and pursue efforts to limit the temperature increase to 1.5°C as much as possible, with greenhouse gas (GHG) emissions reaching net zero by the latter half of the 21st century. In response to these international trends, the IMO agreed with the Marine environment protection committee (MEPC) meeting held in London in 2018 to set emission reduction targets for the shipping industry, including reducing total GHG emissions by more than 50% by 2050 compared with 2008 levels. This marked the shipping industry's first international commitment. The IMO has agreed to aim for net-zero GHG emissions as early as possible in this century. Therefore, reducing $CO_2$ emissions through fuel conversion from a long-term perspective is an urgent priority (Ishimaru 2019).

Marine diesel engines are widely adopted as the main auxiliary engines in ships because of their ability to utilize inexpensive heavy fuel oil and their high thermal efficiency as individual units. In the marine sector, research (Takaishi 2015; Izumi 2016; Deng 2025) has been conducted and implemented to reduce fuel consumption and harmful exhaust emissions from medium- and low-speed diesel engines through improvements in supercharging performance, scavenging efficiency, and the introduction of electronic control technology. However, most of these technologies target newly constructed vessels. Examples of research aimed at retrofitting existing engines include oxygen-containing fuels such as water-emulsion fuels (Hiraoka et al., 2016; Woo & Lee 2023) and DME fuels (Fang et al., 2021, Krzeminski & Ustrzycki 2023; Winangun et al., 2023), but their practical implementation remains elusive. Diesel engines are highly durable and expected to operate for extended periods. Therefore, it is necessary to pursue technologies that are applicable to existing engines. In the marine sector, where many vessels are equipped with non-electronically controlled engines, the demand for technologies to reduce fuel consumption and harmful exhaust emissions from existing engines is high.

However, the use of biodiesel fuel is being promoted, primarily for transport vehicles, to reduce energy consumption and environmental impact. Investigations have been conducted on the physicochemical properties of biodiesel fuel when

microbubbles are introduced (Asbanu et al., 2025). Furthermore, studies have been conducted on the engine performance of two-wheeled tractors using this fuel (Herodian 2025). The results confirmed an increase in cetane number when fine bubbles were introduced into the fuel. The effects of these fine bubbles on engine output were clarified, and their positive impact was confirmed.

Previously, the authors conducted research on the application of fuel containing air-derived microbubbles mixed with light oil in high-speed diesel engines (Nakatake et al., 2007, Nakatake et al. 2013, Yamashita et al. 2021) and small gas turbine engines (Nakatake et al., 2020), as well as the application of fuel containing microbubbles mixed with heavy oil in high-speed diesel engines. and further investigated the performance improvement of marine diesel engines using high-viscosity C-grade heavy oil heated and mixed with fine bubbles (Kawahara et al., 2023). These studies have clarified the effects of fuel pretreatment with fine bubbles on fuel economy reduction and exhaust gas emissions.

Considering the future transition to biodiesel fuel for various transport engines, including ships, this study examined the impact of incorporating air as fine bubbles into low-sulfur-A heavy oil, in compliance with SOx regulations, on the operating performance of practical marine medium-speed diesel engines.

## METHODOLOGY

### Fuel properties

Figure 1 shows a microbubble injector that generates bubbles in fuel. The microbubble injector used in this experiment was an OK Engineering OKE-MB2L-PF1/2 model composed of SUS304 stainless steel, as shown in Figure 1(a). As shown in Figure 2(b), the fuel enters the microbubble injector through the center of the tube. The fuel flow rapidly expands the cross-sectional area of the tube, causing vortices to form at the corners of the enlarged tube. In addition, air was aspirated from around the entire circumference of the tube. After convergence at the center of the tube, bubbles are generated in the downstream enlarged flow paths.

Prior to conducting this experiment, we investigated the changes in fuel properties when fine bubbles were introduced into the fuel. Figure 2 shows the experimental apparatus used to characterize fuel containing fine bubbles. The heavy oil fuel stored in a drum was transferred using a vortex pump (Nikuni, model 15KLD02Z), passed through a fine bubble introducer, and delivered to a classification tank. The air supply to the fine-bubble injector was adjusted using a flow meter (Azbil Corporation, CMS0002BSRN200000) via a needle valve to achieve a predetermined air volume. This classification tank was designed to allow larger bubbles to rise to the upper section of the tank, whereas smaller bubbles flowed into the primary fuel stream. The fuel containing fine

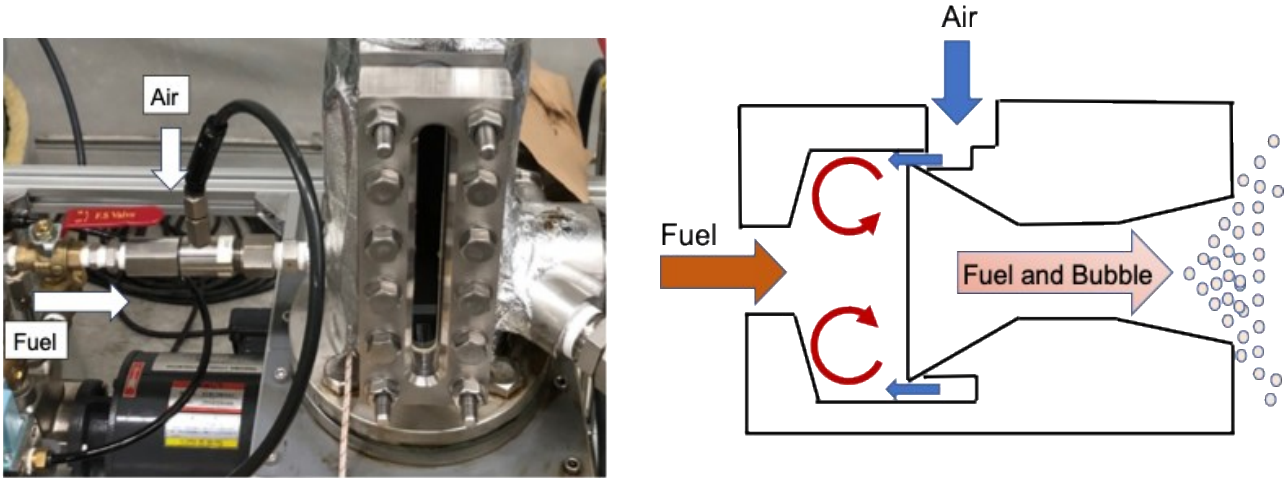


(a) Detail drawing of mixer (b) Flow structure in mixer

Figure 1. Micro bubble mixer

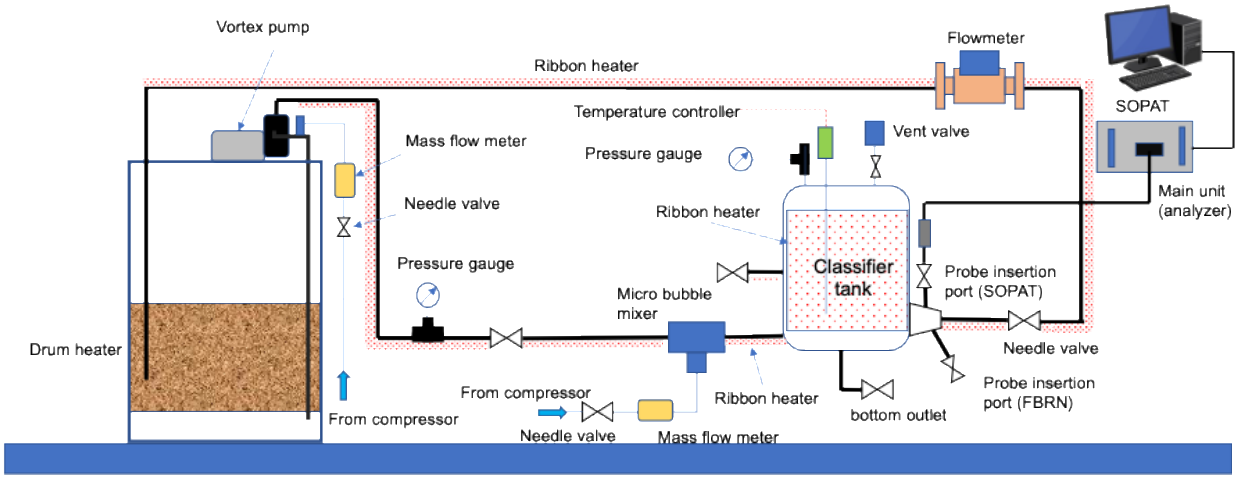


Figure 2. Experimental equipment for fuel oil properties

Table 1. Properties of fuel used

| Test items | Unit | A-grade heavy oil | C-grade heavy oil |
|---|---|---|---|
| Density | g/cm$^3$ | 0.8532 | 0.9618 |
| Flash point | mm$^2$/s | 69.0 | 95.0 |
| Kinematic viscosity | ℃ | 1.921 | 90.1 |
| Flow point | ℃ | -25 | -20 |
| Moisture (distillation method) | Volume % | 0.00 | 0.00 |
| Residual carbon content | Mass % | 0.52 | 10.2 |
| Ash | Mass % | 0.00 | 0.015 |
| Sulfur content | Mass % | 0.075 | 2.25 |
| Reaction | | Neutral | Neutral |
| Nitrogen content | Mass % | Less than 0.01 | 0.18 |
| Gross calorific value | kJ/kg | 45,490 | 43,260 |

bubbles exiting the classification tank was passed through a flow meter and returned to the original drum. The heaters were wrapped around the drum, fuel piping, and classification tank within the experimental apparatus to enable precise temperature control. This allowed to conduct experiments using high-viscosity C-grade heavy oils. To investigate the characteristics of the bubbles in the fuel fed from a fine-bubble injector, the particle size and size distribution were measured from the particle image data using a probe-type image analysis system (SOPAT Microscopic MM-2). The probe was then inserted into the main outlet of the classification tank for observation. For the fuel property measurements, samples were extracted from the bottom of the classification tank to determine the specific gravity and viscosity of the fuel. Table 1 lists the main fuel properties and compositions used in the experiment. Figure 3 shows the results of capturing the behavior of fine bubbles in fuel using a probe-type image-analysis device. As shown in Figure 3 (a), when no fine bubbles were introduced into the fuel, Heavy Oil A appeared brownish red, but changed to a cloudy white color when fine bubbles were introduced. Furthermore, the fine bubbles in the fuel were captured using a probe-type image analysis device, as shown in the figure. Using the image data captured at a rate of 15 Hz, the particle-size distribution of the fine bubbles was calculated, and the results are shown in Figure 3(b). This figure confirms that bubble diameters ranging from 5 to 95 μm were observed at the outlet of the classification tank, with an average bubble diameter of 38 μm. Next, for fuel property measurements, this study investigated fuel properties when fine bubbles were introduced into C heavy oil at varying heating temperatures to

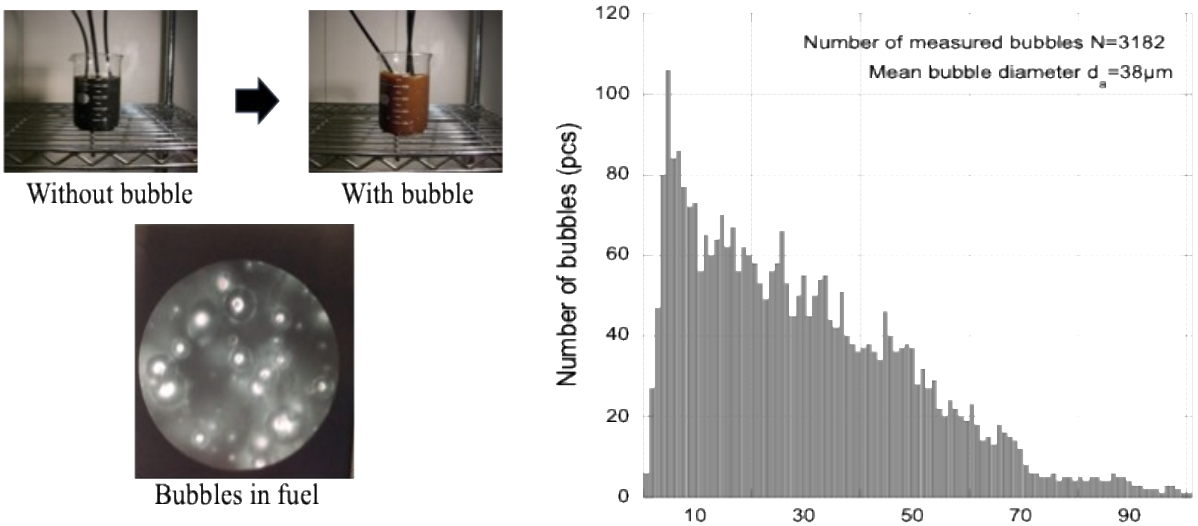


(a) Observation of bubble in fuel

(b) Bubble characteristics in fuel

Figure 3. Bubble behavior in fuel

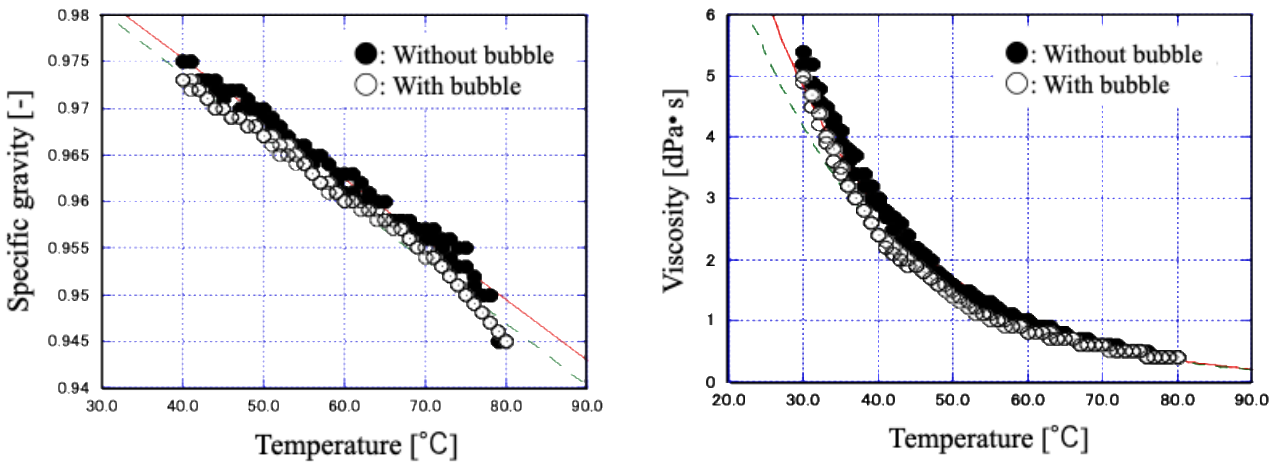


(a) Specific gravity

(b) Viscosity

Figure 4. Fuel oil properties with and without microbubbles

understand fine bubble characteristics over a wide range. Figure 4 shows changes in the specific gravity and viscosity of C heavy oil heated from 40°C to 80°C with and without fine bubbles. For the specific gravity shown in Figure 4(a), it decreases linearly overall with increasing temperature. Furthermore, incorporating fine bubbles into the fuel generally reduces the specific gravity. This trend becomes more pronounced at higher temperatures, with a 2% reduction observed at a fuel temperature of 75°C. Next, the viscosity shown in Figure 4(b) decreases curvilinearly overall with increasing temperature. Incorporating fine bubbles into the fuel also reduces the viscosity across the entire temperature range, with a 15% reduction confirmed at a fuel temperature of 40°C.

## Test engine

The diesel engine used in this study was a marine medium-speed, four-stroke diesel engine (Matsui Tekkou, MU323DGSC), as shown in Figure 5. The specifications are listed in Table 2.

Figure 5. Overview photograph of test engine

Table 2. Specifications of test engine

| | |
|---|---|
| Manufacturer | Matsui Tekkojo Co., Ltd. |
| Model name | MU323DGSC |
| Model | Medium speed 4-stroke diesel engine turbocharger with air cooler |
| Number of cylinders | 3 |
| Cylinder diameter | 230mm |
| Stroke | 380mm |
| Connecting rod length | 751mm |
| Continuous maximum output | 257.4kW (350.0PS) |
| Number of revolutions | 420rpm |
| Net mean effective pressure | 1.77MPa |
| Compression ratio | 13 |
| Intake valve open/close | BTDG 66deg/ABDC 35deg |
| Exhaust valve open/close | BBDC 80deg/ATDC 35deg |
| Injection nozzle | φ0.32mm×7 |
| Fuel | A-grade heavy oil |

For exhaust gas measurements, a combustion gas analyzer (Testo, Testo350) was used to measure the NOx, $O_2$, and $CO_2$ concentrations. The smoke value was measured using an optical transmission opacimeter (AVL Dismoke4800) compliant with JIS D 8005. For both the combustion gas analysis and smoke value measurement, probes were inserted for a fixed period into the probe insertion port located on the flange of the exhaust duct, positioned 2 m downstream from the engine supercharger outlet. Figure 6 shows the fuel supply piping diagram of the engine used for conducting the engine performance tests. Although this test engine was built according to A-grade heavy oil specifications, this testing facility is equipped to select either A heavy oil or C heavy oil as fuel. Fuel is delivered to the service tank, fuel oil measurement tank, and mixing tank. It is then sent

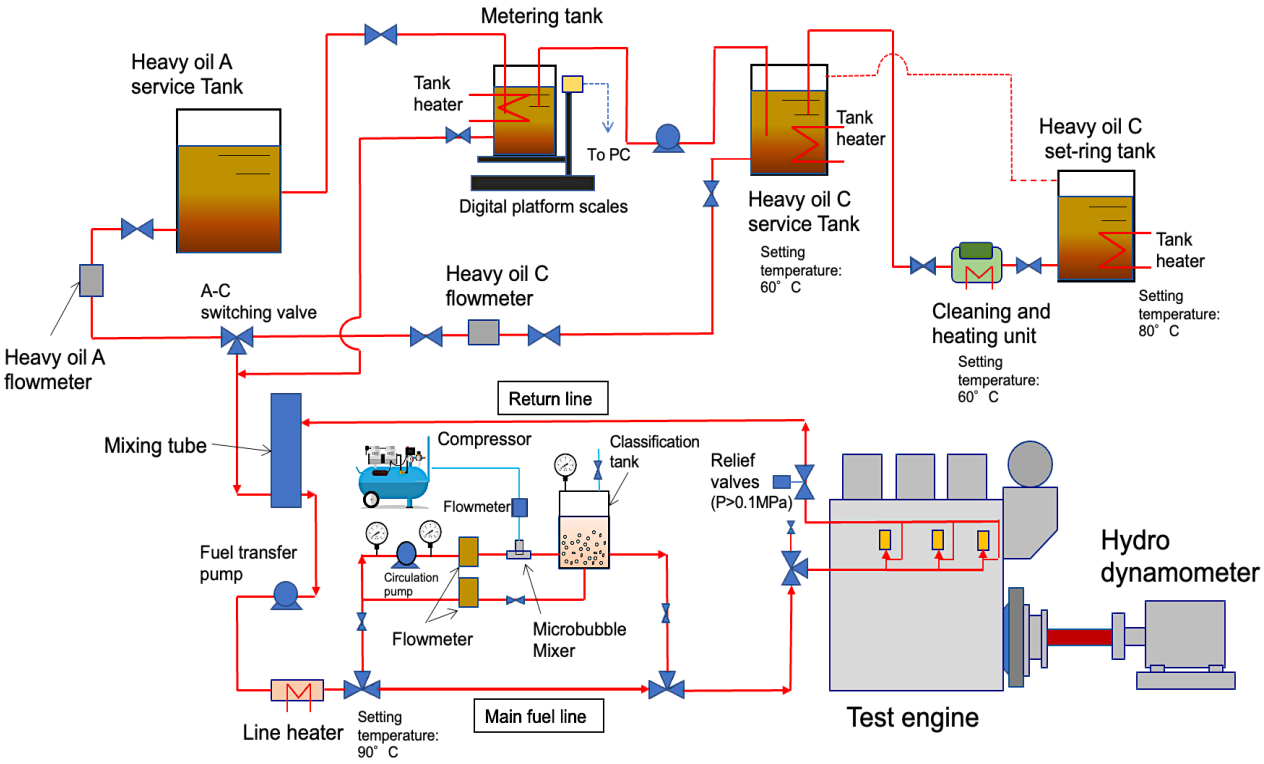


Figure 6. Fuel system diagram of test engine

from the fuel supply pump through the main fuel line to each fuel injection pump of the engine. When supplying microbubbles, after passing through the fuel supply pump, the fuel flows to the bypass line side of the three-way valve. After passing through the circulation pump and fuel flow meter, bubbles are introduced into the fuel at the microbubble injector. A specified air flow rate is supplied to the fine bubble injector via a compressor. A classification layer is installed downstream of the fine bubble injector to supply only bubbles smaller than 40μm to the engine side. Ultimately, the main fuel is supplied to the engine side. However, any excess fuel not sent to the fuel injection pumps due to fuel adjustment is directed to the mixing tank mentioned earlier.

In this experiment, to precisely measure the engine fuel consumption, fuel from heavy oil service tank A was first sent to the heavy oil metering tank. The fuel consumption during engine operation was measured using an electronic scale, and the time-series data were displayed on a computer.

### Experimental method

In the engine performance testing, two fuels were used: one without entrained microbubbles and the other with microbubbles, where the entrained air volume varied. The load rates were set to 25%, 50%, 75%, and 87.5% (the maximum load rate achievable for this engine as a 100% load could not be adjusted). The effects of fuel type (Figure 7) show the timetable for the engine performance tests. After the engine startup, a running operation was performed. Once the state variables of each engine component were confirmed to be stable, the load rate for the test conditions was adjusted. The test transitioned from a state without fine-bubble injection to one with fine-bubble injection, and then proceeded to the next test condition.

## RESULT AND DISCUSSION

### Fuel behavior in fuel piping due to microbubble entrainment

Figure 8 shows the time-series data of pressure and flow rate changes in various sections of the fuel piping after the experiment began. In this

experiment, after engine start-up, the engine load was changed from idle to 25%, 50%, 75%, and 87.5%, while the amount of air supplied as fine bubbles in the fuel was randomly varied from 0.2 to 0.4. The measured parameters were six items: fuel flow rate circulating in the fuel line, air discharge volume from the classification tank, air supply volume to the fine bubble injector, inlet and outlet pressures of the circulation pump, and pressure inside the classification tank. When fine air is introduced into the fuel, the air flow rate fluctuates due to pressure variations in the main fuel line, and this tendency increases with rising engine load. Immediately after engine start-up, no significant fluctuations were observed in the circulation pump inlet pressure, but the circulation pump outlet pressure and the pressure inside the separator fluctuated greatly. Subsequently, after adjusting the engine load from idle to 25%, the respective pressure fluctuations decreased.

**Fuel consumption**

Next, this study examined the performance characteristics of the engine. Figures 9 and 10 show the relationships between the engine load and fuel consumption and between the engine load and fuel consumption rate, respectively. The figures also include the results for fuel containing microbubbles with air mass $Q_a$ ranging from 0.1 to 0.3 L/min. Regardless of the presence of microbubbles, fuel consumption increased linearly as the load increased. When fine bubbles were introduced into the fuel, the fuel consumption decreased with increasing load. The effect of introducing fine bubbles on fuel consumption showed no significant change at 25% load, but the fuel consumption decreased as the load increased. These trends are similar to the engine characteristics when using C heavy oil (Kawahara et al. 2023). Under the operating conditions tested, fuel consumption changes began to appear at an air injection rate $Q_a$ of 0.1 L/min. However, at $Q_a \geq 0.4$ L/min, incomplete combustion occurs within the cylinder, leading to instability. Regarding the effect of the air injection rate $Q_a$ on the microbubble injector, the reduction in combustion consumption increased with the load. The greatest reduction effect was observed at a load of 75% and $Q_a$ = 0.3 L/min, achieving a reduction of approximately 4.5%.

**Exhaust gas characteristics**

Figure 11 shows the relationship between the engine load rate and the $CO_2$ and NOx emissions. The air mass flow rate $Q_a$ when fine bubbles were introduced into the fuel was 0.1 to 0.3 L/min. First, $CO_2$ generally increases with an increase in load. When fine bubbles were introduced into the fuel, no significant changes were observed up to a 50% load. However, at loads of 75% or higher, the effect of the air mass $Q_a$ becomes significant. At $Q_a$ = 0.3 L/min and a load of 87.5%, the $CO_2$ emissions were reduced by approximately 10.5% compared to when no fine bubbles were

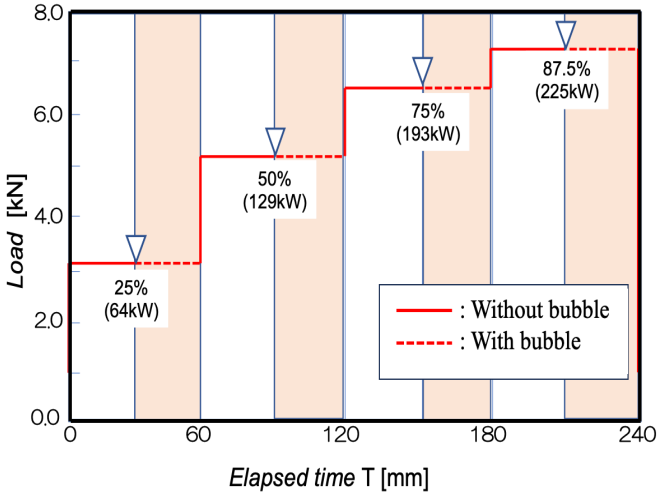


Figure 7. Timetable of experimental conditions for engine performance testing

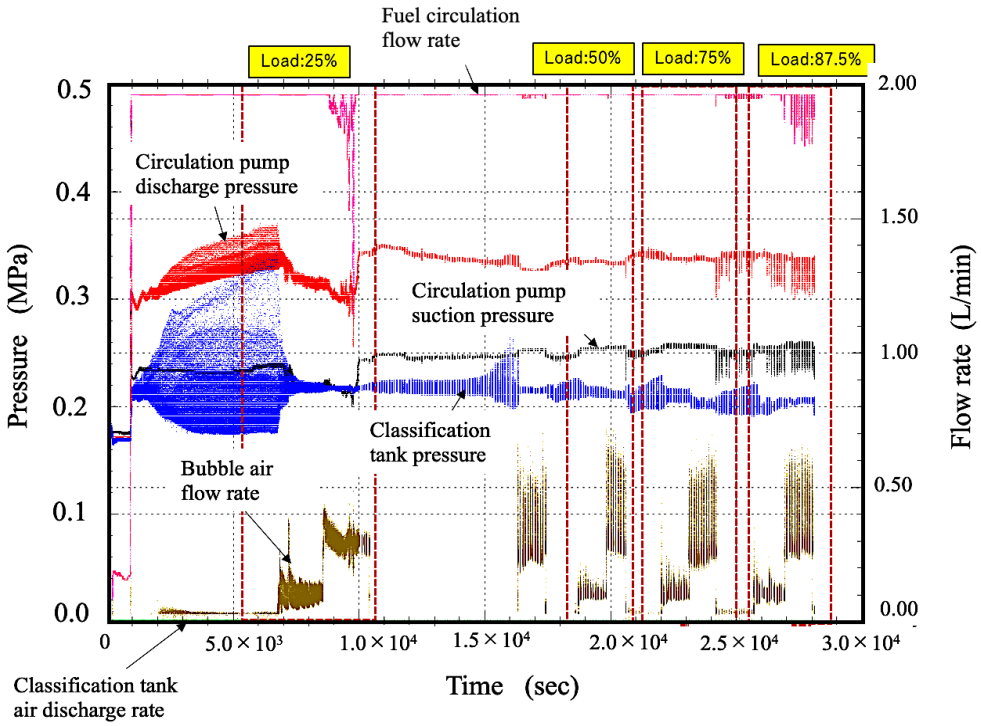


Figure 8. Behavior in fuel piping during operation

introduced. Conversely, NOx showed an increasing trend with increasing load when no fine bubbles were introduced. However, when fine bubbles were introduced into the fuel, a decrease in NOx was confirmed at $Q_a$ =0.2 and 0.3 L/min when the load exceeded 75%. This trend in NOx change with increasing load was found to differ from the results previously obtained for C heavy oil.

Figure 12 shows the relationship between the engine load rate and smoke value. Note that the air quantity $Q_a$ when fine bubbles are introduced into the fuel is 0.1 to 0.3 L/min. For fuel without fine bubbles introduced, the smoke value was 0.17 $m^{-1}$ at 25% load. It decreased to 0.08 $m^{-1}$ at 50% load, then increased slightly with increasing load, before turning downward again at 87.5% load. Next, when fine bubbles are introduced into the fuel, the trend in the smoke value changes with increasing load and is similar to that without fine bubbles; however, the smoke value itself decreases across all loads. The largest reduction occurred at an airflow rate $Q_a$ of 0.3 L/min, showing a decrease in smoke value at all loads compared to any other airflow rate, with a maximum reduction of approximately 34% at an 87.5% load. This trend in smoke change is almost identical to the results for heavy oil.

## Cylinder internal pressure and heat generation rate

By introducing fine bubbles into the fuel, differences were observed in the operating characteristics and exhaust gas properties of the engine. Therefore, we investigated the combustion state within the cylinder, specifically, the cylinder pressure and heat generation rate. Figure 13 shows the relationship between the cylinder pressure and heat generation rate versus the crankshaft angle when the engine load rate is varied. The figure also includes results for air mass $Q_a$ of 0.1 to 0.3 L/min when fine bubbles were introduced into the fuel. Regarding the cylinder pressure changes, ignition was observed at all engine loads and with all fuels, followed by a rapid pressure increase and a subsequent transition into the afterburning period. Notably, incorporating fine bubbles into the fuel slightly reduced the maximum cylinder pressure change and delayed the ignition. Although this ignition delay period was expected to prolong the subsequent afterburning period, the afterburning duration matched that of fuel without fine bubbles. Subsequently, the heat generation rate was calculated from the cylinder pressure change versus the crankshaft angle. The heat generation rate,

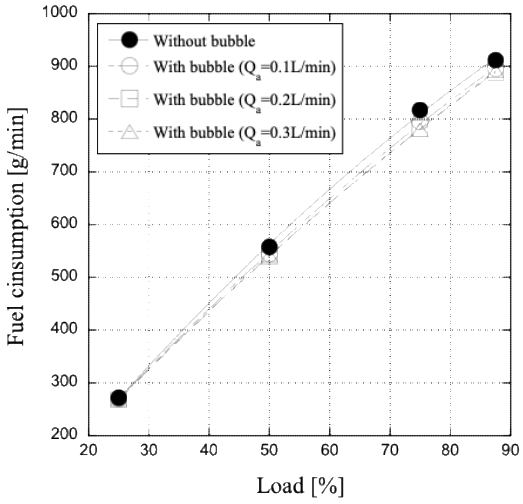


Figure 9. Relationship between engine load and fuel consumption

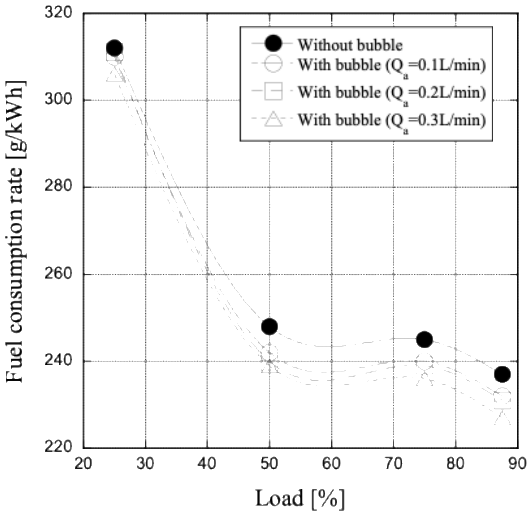


Figure 10. Relationship between engine load and fuel consumption rate

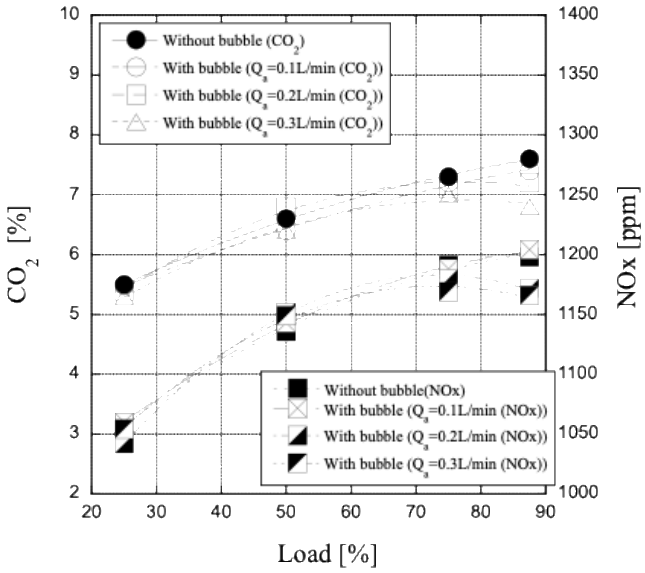


Figure 11. Relationship between engine load and $CO_2$

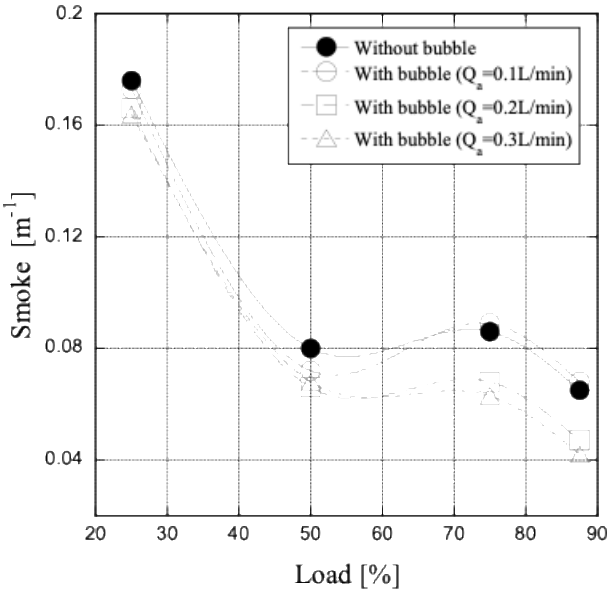


Figure 12. Relationship between engine load and smoke level

which is similar to the cylinder pressure change, increases sharply simultaneously with fuel ignition. For the fuel with fine bubbles, the increase in the heat generation rate was delayed compared to the fuel without fine bubbles owing to the delayed ignition period. However, the peak value of the heat generation rate was higher than that of fuel without fine bubbles. It was found that the changes in the cylinder pressure and heat generation rate exhibited similar trends at all loads. Next, based on the results in Figure 13, the maximum cylinder pressure change relative to crank angle, peak heat generation rate, and ignition delay period were organized for each load condition. Figure 14 shows the relationship between the air supply rate $Q_a$, the microbubble injector, the maximum cylinder pressure, and the peak heat generation rate at a representative 75% load. First, the maximum cylinder pressure decreased as the air mass $Q_a$ increased but showed a slight increase when $Q_a$ = 0.3 L/min. In contrast, the peak heat generation rate increases with increasing air mass $Q_a$, which differs from the change in the maximum cylinder pressure, and shows a slight decrease at $Q_a$ = 0.3 L/min. Figure 15 shows the ignition timing retraction period based on the cylinder pressure versus the crank angle shown in Figure 13, using the value for the fuel without fine bubbles as a reference. As shown in the figure, introducing fine bubbles into the fuel retracted the ignition delay period at all loads, and this retraction increased with increasing load. At an airflow rate $Q_a$ of 0.1 L/min to the microbubble mixer, the onset of the ignition delay increased sharply as the load increased from 25% to 50%. However, at loads above 50%, the delay angle stabilizes at approximately -1.4 to -1.5 degrees. Furthermore, when the air flow rate $Q_a$ is 0.2 L/min, the onset of ignition delay is greater than when $Q_a$ is 0.1 L/min from 25% to 50% load, and the onset delay also increases beyond 50% load. Furthermore, at an air flow rate $Q_a$ of 0.3 L/min, the trend from 25% to 50% load is similar to that at $Q_a$ = 0.2 L/min, but beyond 75% load, the retard angle increases further, reaching -2.8 degrees at 87.5% load. These changes are similar to the experimental results obtained for high-speed diesel engines (Yamashita et al. 2021) and for medium-speed diesel engines using C heavy oil (Kawahara et al., 2023).

Based on the above, the inclusion of fine bubbles in the fuel alters the compressibility of the fuel within the fuel injection pump, thereby increasing the work required for compression. Consequently, this likely caused a delay in fuel injection timing. In other words, it can be inferred that the ignition delay was caused by an overall shift in the ignition delay period and not by a decrease in fuel ignitability. The decrease in the

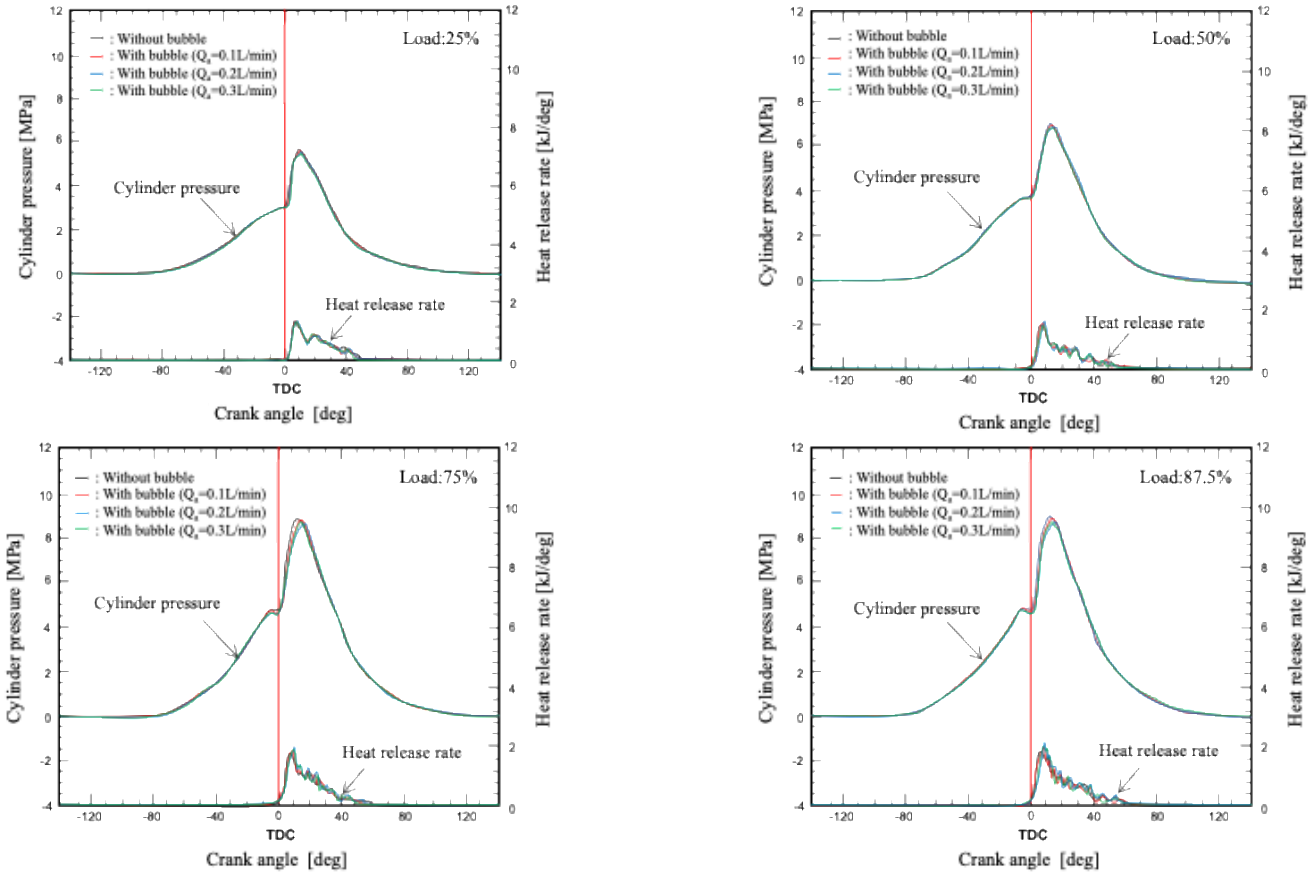


Figure 13. Relationship between in-cylinder pressure and heat release rate versus crank angle

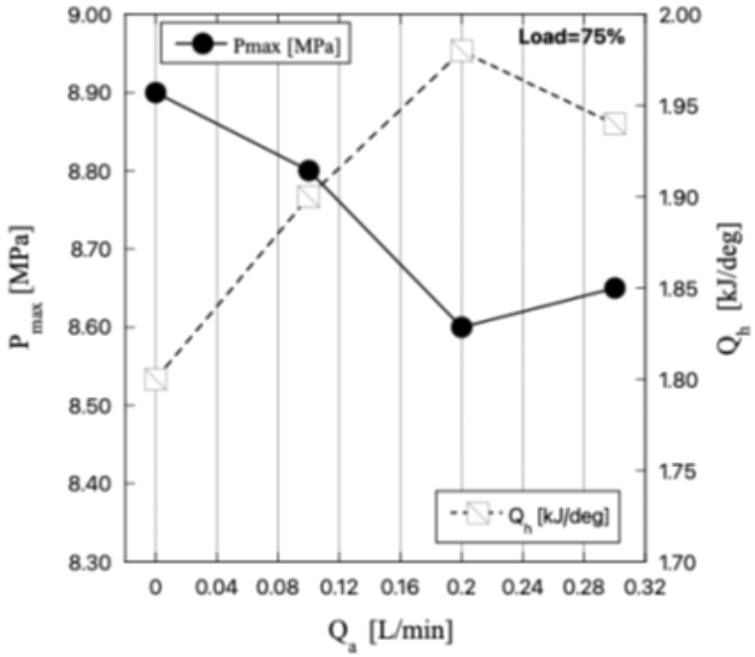


Figure 14. Relationship between in-cylinder pressure and heat release rate at 0-60 degrees crank angle with 75% engine load

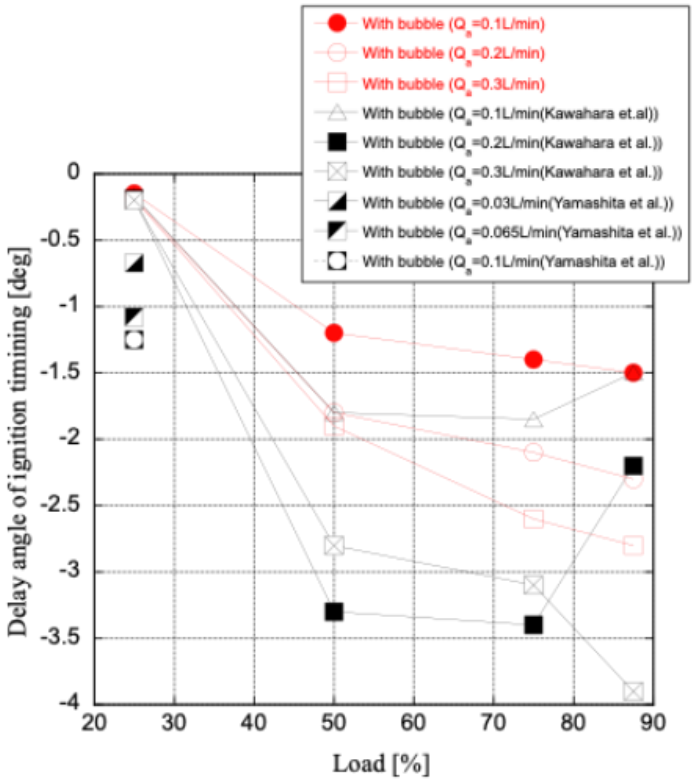


Figure 15. Influence of microbubbles on the delay angle of ignition timing

maximum cylinder pressure was likely due to both the delayed ignition caused by the later fuel injection timing and the reduced fuel injection quantity. When ignition was delayed, premixed combustion occurred after the cylinder volume expanded, leading to a lower maximum cylinder pressure. Delayed injection timing prolongs the afterburning period, but experimental results show no change in the afterburning duration. Therefore, it is considered that the fuel injection quantity decreased due to air entrainment in the fuel. Furthermore, the increase in the maximum heat release rate when fine bubbles were introduced into the fuel is attributed to improved premixed combustion due to fuel atomization, which in turn enhanced the pressure rise rate within the cylinder. The delayed peak position of the maximum heat release rate is considered to result from delayed ignition caused by the delayed injection timing. Furthermore, the reason fuel consumption changes with the amount of air $Q_a$ introduced into the fuel is that at an air flow rate $Q_a$ of 0.1 L/min, insufficient fine bubbles are introduced into the fuel, and at $Q_a$ of 0.4 L/min or higher, many of the generated fine bubbles rise and separate within the classification layer. Therefore, when the air flow rate $Q_a$ is 0.3 L/min, the amount of bubbles introduced into the fuel is maximized. Based on the results in Figure 13, this is expected to reduce the maximum value of the cylinder pressure change while conversely improving the heat release rate. For these reasons, under the experimental conditions of this study, the air flow rate $Q_a$ of 0.3 L/min to the fine bubble introducer demonstrated the best engine performance. Finally, based on these results, the effect of adding microbubbles to A hevary fuel oil used in medium-speed marine diesel engines on engine performance has been clarified. However, because the engine employed mechanical fuel injection timing, experiments varying the fuel injection timing could not be conducted. In the future, we plan to modify the engine to enable variable fuel-injection timing. Using conventional fuel without fine bubbles and with consistent fuel injection timing, we conducted experiments to confirm the validity of the above observations.

## CONCLUSION

A study was conducted on the combustion characteristics and exhaust gas properties of medium-speed marine diesel engines when introducing fine bubbles into A-grade heavy oil. The following conclusions were obtained. When fine bubbles were introduced into the fuel, poor combustion and engine instability occurred across the entire load range where $Q_a$ was 0.4 L/min or higher. However, at $Q_a$ values below 0.4 L/min, fuel efficiency improvement increased significantly with increasing load, achieving a maximum reduction of 4.5% at 75% load and $Q_a$ = 0.3 L/min. Regarding exhaust gas characteristics, no significant changes were observed at low load ranges for different fine bubble injection rates. However, at loads of 75% or higher, both $CO_2$ and NOx emissions decreased as the microbubble injection rate increased. Furthermore, injecting microbubbles into the fuel promoted atomization after fuel injection, similar to the case with heated C heavy oil, improving the heat release rate across the entire engine load range.

## ACKOWLEDGEMENT

This research was conducted under the Strategic Energy-Saving Technology Innovation Program (Development of a Marine Internal Combustion Engine Fuel Efficiency Improvement Device Using Microbubbles) of the Japan Project for New Energy and Industrial Technology Development Organization (NEDO) grant-in-aid program (JPNP12004). We express our gratitude for your comment.

## GLOSSARY OF TERMS

| Symbol | Definition | Unit |
|---|---|---|
| IMO | International maritime organization | |
| NOx | Nitrogen oxides | ppm |
| SOx | Sulfur oxides | |
| PM | Particulate matter | |
| COP21 | 21st conference of the parties | |
| UNFCCC | United Nations Framework Convention on Climate Change | |
| GHG | Greenhouse gas | |
| MEPC | Marine Environment Protection Committee | |
| $O_2$ | oygen | |
| $CO_2$ | carbon dioxide | % |
| $Q_a$ | air flow rate | L/min |
| NEDO | New Energy and Industrial Technology Development Organization | |

## REFERENCES

Asbanu, H., Herodian, S., Mandang, T., Sugiarto, A. T., & Anggarani, R. (2025). Physicochemical Properties of B-0 CN 51 Diesel Fuel with Ultrafine Bubbles. Scientific Contributions Oil and Gas, 48(1), 31-42. https://doi.org/10.29017/scog.v48i1.1686

Deng, B., Cai, W., Zhang, W., Bian, L., Che, X., Xiang, Y., & Wu, D. (2025). A comprehensive investigation of EGR (exhaust gas recirculation) effects on energy distribution and emissions of a turbo-charging diesel engine under World Harmonized transient cycle. Energy, 316, 134506.

Elkelawy, M., Alm-EldinBastawissi, H., El Shenawy, E., & Ouda, M. M. (2025). A Greening the Diesel: Vegetable Oil Biodiesel Blends for Cleaner Emissions and Improved Direct Injection Diesel Engine performance. Journal of Engineering Research, 8(6), 16.

Fang, J., Liu, Y., Wang, K., Shah, H. R., Mu, S., Lang, X., & Wang, J. (2021). Sooting tendency analysis of oxygenate-diesel blended fuels by the affecting indicators of carbon number, oxygen content and H/C ratio. Fuel, 290, 119789.

Hiraoka, N., Miyanagi, A., Kuroda, K., Ito, K., Nakagawa, T., & Ueda, T. (2016). The world's first onboard verification test of UE engine with low pressure EGR complied with IMO's NOx

tier III regulations. Mitsubishi Heavy Ind. Tech. Rev, 53(2), 40-47.

Herodian, S. (2025). Effect Of Adding Ultra Fine Bubble To Diesel And Biodiesel Fuel On Two Wheel Tractors Diesel Engine Performance. Scientific Contributions Oil and Gas, 48(1), 19-29. https://doi.org/10.29017/scog.v48i1.1685

Izumi, Y. (2016). Development History of Yanmar's Marine Medium Speed Diesel Engines, J. JIME, 51-5.

Ishimaru, M. (2019). Fuel Conversion Trends in the Shipping Industry and Potential of Electric Power Propulsion Ships, Kyosai Souken Rep. 162, 68-75.

IMO. (2022). International Convention for the Prevention of Pollution from Ships (MARPOL) Annex VI, International Maritime. Organization (IMO).

Kawahara H., Uemura N., Yamashita H., Nakatake Y., Terasaka K., Kawahara H. & Goto H. (2023). Combustion and Exhaust Gas Characteristics of Residual Oil Mixed with Air-Fine Mixture in Medium-Speed Marine Diesel Engine, J. JIME, 58(2): 128-136.

Krzemiński, A., & Ustrzycki, A. (2023). Effect of ethanol added to diesel fuel on the range of fuel spray. Energies, 16(4), 1768.

Nakatake, Y. (2007). Combustion improvement for diesel engines with ejector-type micro-bubble mixed fuel. Transactions of Japan Society of Mechanical Engineers, Series B, 73(735), 196-202.

Nakatake, Y., Kisu, S., Shigyo, K., Eguchi, T., & Watanabe, T. (2013). Effect of nano air-bubbles mixed into gas oil on common-rail diesel engine. Energy, 59, 233-239.

Nakatake, Y., Yamashita, H., Tanaka, H., Goto, H., & Suzuki, T. (2020). Reduction of fuel consumption of a small-scale gas turbine engine with fine bubble fuel. Energy, 194, 116822.

Takaishi, T. (2015). Approach to High Efficiency Marine Low Speed Diesel Engine, J. JIME, 50-2.

Woo, S., & Lee, K. (2023). Effect of injection strategy and water content on water emulsion fuel engine for low pollutant compression ignition engines. Fuel, 343, 127809.

Winangun, K., Setiyawan, A., & Sudarmanta, B. (2023). The combustion characteristics and performance of a Diesel Dual-Fuel (DDF) engine fueled by palm oil biodiesel and hydrogen gas. Case Studies in Thermal Engineering, 42, 102755.

Yamashita H., Kudo T., Nakatake Y., Tanaka H., Kawahara H., Terasaka K., Kawahara H. & Goto H. (2021). Reducing Fuel Consumption and NOx Emissions from High-speed Diesel Engine with Air Fine Bubble A-heavy Oil, J. JIME, 56(4), 152-158.